NIH Public Access
Author Manuscript
Magn Reson Med. Author manuscript; available in PMC 2015 January 01.

Published in final edited form as:
Magn Reson Med. 2014 January ; 71(1): . doi:10.1002/mrm.24669.

Non-contrast Skeletal Muscle Oximetry

Zheng Jie[1], **Hongyu An**[2], **Andrew R. Coggan**[1], **Xiaodong Zhang**[3], **Bashir Adil**[1], **David Muccigrosso**[1], **Linda R. Peterson**[1], and **Robert J. Gropler**[1]

[1]Mallinckrodt Institute of Radiology, Washington University School of Medicine, St. Louis, Missouri, USA

[2]University of North Carolina, Chapel Hill, North Carolina, USA

[3]Department of Radiology, Peking University First Hospital, 8 Xishiku Street, Beijing, China

Abstract

Purpose—The objective of this study was to develop a new non-contrast method to directly quantify regional skeletal muscle oxygenation.

Methods—The feasibility of the method was examined in five healthy volunteers using a 3T clinical MRI scanner, at rest and during a sustained isometric contraction. The perfusion of skeletal muscle of the calf was measured using an arterial spin labeling method, whereas the oxygen extraction fraction of the muscle was measured using a susceptibility based MRI technique.

Results—In all volunteers, the perfusion in soleus muscle increased significantly from 6.5 ± 2.0 ml/100g/min at rest to 47.9 ± 7.7 ml/100g/min during exercise ($P < 0.05$). While the corresponding oxygen extraction fraction did not change significantly, the rate of oxygen consumption increased from 0.43 ± 0.13 to 4.2 ± 1.5 ml/100g/min ($P < 0.05$). Similar results were observed in gastrocnemius muscle, but with greater oxygen extraction fraction increase than the soleus muscle.

Conclusion—This is the first MR oximetry developed for quantification of regional skeletal muscle oxygenation. A broad range of medical conditions could benefit from these techniques, including cardiology, gerontology, kinesiology, and physical therapy.

Keywords

Cardiovascular Magnetic Resonance; Arterial Spin Labeling; Skeletal Muscle; Oxygen Consumption; Oxygen Extraction Fraction

INTRODUCTION

Skeletal muscle is the largest single tissue in the body, accounting for ~40% of body mass and about one-third of resting energy expenditure (1). Moreover, skeletal muscle is unique among tissues in that its demand for energy can rapidly increase 10–50 fold, or even more, during contractile activity. The coupling of skeletal muscle O_2 consumption to mitochondrial ATP synthesis and ultimately to the production of useful work (e.g., force generation at the myofibrillar level) is therefore a very important determinant of both the overall energy needs of the body as well as the capacity to perform physical exercise.

Correspondence to: Jie Zheng, PhD, Mallinckrodt Institute of Radiology, Box 8225, Washington University School of Medicine, 510 South Kingshighway Blvd., St. Louis, MO63110, USA, Tel: 314-747-4608; fax: 314-747-3882.

NIH-PA Author Manuscript
NIH-PA Author Manuscript
NIH-PA Author Manuscript

NIH-PA Author Manuscript

NIH-PA Author Manuscript

NIH-PA Author Manuscript

Given the above, it is noteworthy that mitochondrial coupling and/or the efficiency of muscle contraction have been reported to be altered in a variety of physiological and pathological states, e.g., obesity (2), aging (3,4,5,6), heart failure (7,8). Patients with heart failure, for example, exhibit increased O_2 consumption and thus reduced whole-body gross efficiency during exercise, presumably reflecting a reduction in the overall efficiency of skeletal muscle production/utilization of ATP. However, other studies (9,10) have concluded that mitochondrial coupling and/or muscular efficiency are unaltered in these conditions. Such inconsistent results may stem from limitations of available methods for determining regional skeletal muscle O_2 consumption *in vivo*. Historically, this has required either performing arterio-venous balance measurements to directly quantify limb O_2 consumption (11), or inferring changes in skeletal muscle O_2 consumption from changes in whole-body O_2 consumption during exercise (12). The former approach is too invasive for routine use, whereas the latter may be too insensitive to reliably detect differences in muscle metabolism in patients with a low absolute exercise capacity. More recently, other approaches have been employed, such as near-infrared spectroscopy (NIRS) (13) or positron emission tomography (PET) using $^{15}O_2$ as a tracer (14). With NIRS, however, it is difficult to quantify the absolute rate of O_2 consumption and there is limited penetration in deep muscle tissue, while with PET the subject must be exposed to ionizing radiation and injected with radioactive isotopes.

Several attempts have been made to assess regional muscle O_2 status using cardiovascular magnetic resonance imaging (CMR) via the blood-oxygen level dependent (BOLD) effect (15,16,17,18,19) or on large veins (20). However, traditional BOLD imaging only provides a qualitative measure of tissue O_2 change. Elder CP et al (21) applied an empirically determined relationship between R2′ and hemoglobin O_2 saturation (%HbO_2) to estimate regional %HbO_2. They have successfully quantified this index and demonstrate very good agreement with measurement results using NIRS modality.

In this study, we evaluated a newly developed MRI muscle oximetry approach for measuring regional skeletal muscle oxygen extraction fraction (SMOEF) without using any *in vitro* calibration. The study was performed in normal volunteers who underwent leg exercise during the MRI scans. Skeletal muscle leg blood flow (SMBF) was also quantified for the calculation of O_2 consumption rate in skeletal muscle ($SMVO_2$).

METHODS

MRI Methods

The approach to measuring $SMVO_2$ is based on Fick's principle:

$$SMVO_2=[O_2]\times Y_a\times SMOEF\times SMBF \quad [1]$$

where the constant $(O_2)_a$ is the total oxygen content of arterial blood (assumed = 7.99 μmol/ml); and Y_a is the oxygen saturation in arterial blood. All imaging was performed using a 3T Trio Siemens whole-body MR system (Siemens Medical Solution, Malvern, PA) and a home-made flexible surface coil for signal receiver.

The measurement of SMOEF was derived from a model (22) used to calculate brain tissue oxygen extraction fraction with the magnetic susceptibility effect on deoxyhemoglobins (23,24). A multi-slice 2D triple-echo asymmetric spin-echo sequence was implemented to acquire source images for the model, although only one slice was obtained in this study (Fig. 1). The time intervals between the 90° and 180° pulses and between 180° and the echo center (k space center) were defined as t_1 and t_2. If the 180° pulse has a time offset (τ) from TE/2, t_1 and t_2 become TE/2−τ and TE/2+τ, respectively. In this case, an asymmetric spin

NIH-PA Author Manuscript

NIH-PA Author Manuscript

NIH-PA Author Manuscript

echo will be formed, in which a special transverse relaxation rate R_2' (= $R_2 - R_2$*) decay time will be 2τ. In total, triple-echo asymmetric spin echo images were acquired with three $TE_1/TE_2/TE_3$ =44/62/80 ms. There were a total of 46 images with varying τ and the increment of τ was 0.5 ms between two adjacent acquisitions. This acquisition scheme yielded a series of ΔTE (2τ) ranging from (−18 ms, 27 ms), (0, 45 ms), and (18, 63 ms), respectively, for each echo. Of note, the R_2' decay time is |ΔTE|. Other imaging parameters were: TR = 4 s; Field of View (FOV) = 160 × 140 mm^2; matrix size = 64 × 56 and interpolated to 128 × 112; single-slice, slice thickness = 8 mm; total acquisition = 3 min 48 s.

The images were processed based on the model proposed previously (21). Briefly speaking, using an asymmetric spin-echo sequence with different π pulse time offsets while keeping an identical TE for each echo, the measured MR signal can be characterized as:

$$S(t)=\rho(1-\lambda)\cdot e^{-\lambda\cdot f_c(\delta\omega t)}\cdot e^{-\frac{TE}{T_2}} \quad [2]$$

where ρ is the spin density; λ is the volume fraction containing deoxyhemoglobin, representing skeletal muscle venous blood volume; and $f_c(\delta\omega t)$ can be described as:

$$f_c(\delta\omega t)=1/3\cdot\int_0^1(2+u)\cdot\sqrt{1-u}\cdot\frac{1-J_0(\frac{3}{2}\cdot\delta\omega t\cdot u)}{u^2}\mathrm{du} \quad [3]$$

where $J_0(x)$ is the zeroth order Bessel function; and δω is the characteristic frequency shift and is defined as:

$$\delta\omega=\frac{4}{3}\pi\gamma\cdot\Delta\chi_0\cdot\mathrm{Hct}\cdot\mathrm{SMOEF}\cdot B_0 \quad [4]$$

where Hct is the fractional hematocrit; B_0 is the main magnetic field strength; $\Delta\chi_0$ is the susceptibility difference between fully oxygenated and fully deoxygenated blood, which has been measured to be 0.27 ppm per unit Hct in centimeter–gram–second units (25). In this study, a constant Hct of 0.4 was employed for all subjects. Because Eq. 2 cannot be solved analytically, two asymptotic forms, namely short time scale ($\delta\omega\cdot|t|\le 1.5$) and long time scale ($\delta\omega\cdot|t|>1.5$) are given to approximate the signal equation (21) as:

$$S_s(t)=\rho(1-\gamma)\cdot\exp(-0.3\,\lambda\cdot(\delta\omega t)^2)\;\delta\omega\cdot|t|\le 1.5 \quad [5]$$

and

$$S_1(t)=\rho(1-\lambda)\cdot\exp\left(-R_2'(|t|-tc)\right)\delta\omega\cdot|t|>1.5 \quad [6]$$

where the subscript s and l denote the short and long time scales, respectively; t_c is the critical time defined as tc =1/δω. R_2' can be written as:

$$R_2'=\lambda\cdot\delta\omega=\lambda\tfrac{4}{3}\pi\gamma\cdot\Delta\chi_0\cdot\mathrm{Hct}\cdot(1-Y)\cdot B_0. \quad [7]$$

R_2' can be estimated by fitting a straight line of the logarithm of $S_l(t)$ with $t > 1.5/\delta\omega$. λ can be calculated as $\lambda=\ln[S_1(t=0)]-\ln(S_s(t=0))$, where $S_l(t=0)$ can be obtained through an extrapolation of Eq. 6 following the estimation of R_2' (21). After both R_2' and λ are estimated, measurement of SMOEF can be obtained from Eq. 7.

NIH-PA Author Manuscript

NIH-PA Author Manuscript

NIH-PA Author Manuscript

SMBF was determined using an arterial spin labeling (ASL) technique. Similar methods have been widely used in skeletal muscle for quantitative perfusion measurement without injecting contrast agents (20,26,27,28). In this study, we adapted an ASL method validated in the myocardium for use in skeletal muscle, which was reported previously in detail (29). Briefly speaking, the acquisition sequence is an inversion recovery prepared single-shot gradient-echo sequence with slice-selective inversion (SS) and nonselective inversion (NS) acquisitions (30). Tissue T_1 was measured using T_1-weighted images at multiple TI's. SMBF was calculated using the following equation (31):

$$SMBF=\rho\frac{T_{1,NS}}{T_{1,Blood}}\left(\frac{1}{T_{1,SS}}-\frac{1}{T_{1,NS}}\right) \quad [8]$$

where ρ is the constant blood-tissue partition coefficient of water, and ρ = 0.95 ml/g for blood-perfused skeletal muscle tissue (32); $T_{1,NS}$ is the T_1 of the skeletal muscle after the nonselective inversion recovery pulse is applied; $T_{1,Blood}$ is the average T_1 of the arterial blood pool; and $T_{1,SS}$ is the T_1 of the skeletal muscle after the slice-selective inversion recovery pulse is applied. The ASL sequence parameters for the skeletal muscle included: gradient-echo acquisition TR/TE = 2.8 ms/1.2 ms; flip angle = 5°; FOV = 160 × 112 mm^2; matrix = 128 × 90; bandwidth = 650 Hz/pixel; total acquisition = 26 s.

Simulation of SMBF Measurement Errors

A computer simulation was carried out to estimate the impact of signal-to-noise ratio (SNR) on the measurement accuracy of the ASL method. Based on averaged muscle and blood T_1 obtained in our study (not shown), initial T_1 values were assumed: $T_{1,NS}$= 1320 ms, $T_{1,SS}$ = 1300 ms, $T_{1,blood}$ = 1980 ms. Based on resting SMBF found in the literature (see discussion), an averaged resting SMBF of 4.3 ml/100g/min and an exercise SMBF of 43 ml/100g/min (assuming 10-fold increase) were used in the simulation. Signal intensities at different TI were then calculated at two different levels of SMBF with our previously developed algorithm (28). Various levels of Gaussian noise were then added to these signal intensities, followed by the calculation of $T_{1,NS}$, $T_{1,SS}$, and SMBF using Eq. 8. For the sake of simplicity, the $T_{1,blood}$ was fixed at 1980 ms at 3 T. The percentage differences between assumed SMBF and calculated SMBF, i.e., the error of SMBF calculation, were plotted as a function of SNR.

In vivo Experiments

Five healthy volunteers (26 – 52 y, 2F) were recruited and scanned for measurements of calf SMBF, SMOEF, and $SMVO_2$. Signed consent forms were received from all volunteers prior to the imaging sessions. None of them participated in any competitive exercise training. Subjects were instructed to not consume alcohol or perform any moderate to heavy exercise for 24 hour prior to the imaging session. The study was approved by local institutional human study committee. Each volunteer was positioned supine on the MR table with his or her right foot firmly strapped to a pedal of a home-built isometric exercise device (Fig. 2A). The percentage of maximal voluntary contraction (MVC) required during the exercise was estimated based on the torque required to fully depress the pedal of the exercise device in comparison to previous measurements of plantar flexor MVC in healthy but untrained subjects (33). The SMOEF and SMBF measurements were performed at rest and during a sustained static contraction of the calf. Specifically, SMBF and SMOEF measurements started 1.5 min after the start of contraction, resulting in a contraction time of approximately 2.5 min and 6 min, respectively. There were few reports about the steady state time for muscle perfusion and oxygenation during isometric contraction. It was estimated that this steady state time for leg muscle can be reached after 1 to 2 min contraction work (34). To assess the stability of MRI measurements, the same protocol was repeated once to evaluate

NIH-PA Author Manuscript

NIH-PA Author Manuscript

NIH-PA Author Manuscript

the within-session repeatability. Between two measurements, there was a 4-min interval for a break. Furthermore, 3/5 volunteers were recruited back to evaluate the between-day reproducibility. There were no changes in the weight and height for these three volunteers. SMBF and SMOEF measurements were performed once at rest and once during the same exercise protocol.

Data analysis

SMOEF maps were created in a similar fashion as reported in the brain study (2) using home-made software written in Matlab (MathWorks, Natick, MA). $T_{1,NS}$ and $T_{1,SS}$ maps were calculated using an algorithm that accounts for T_1 saturation effects between single-shot gradient-echo acquisitions (28). SMBF map was then obtained using the Eq. 8 with home-made software written in Matlab. Because both soleus and gastrocnemius muscle groups are affected by the sustained contraction, ROI measurements were performed only on these two muscle regions (Fig. 2B and 2C). In fact, these two muscle regions had the highest SNR due to the proximal locations to the surface coil. Other regions, such as tibias anterior muscle, had substantially lower SNR, which will preclude any meaningful measurements. In SMOEF maps, pixels inside the ROI with values of 0 were excluded for analysis. In resting SMBF maps, pixels with values of 0 or greater than 12 ml/100g/min, due to measurement errors and/or macrovascular flow, were also excluded for further analysis. The threshold value of 12 ml/100g/min was approximately the upper limit of measurement error of resting SMBF (~ 2.5 × 4.3 ml/100g/min). $SMVO_2$ data was then subsequently calculated based on Eq. 1 from the ROI values. The within-session repeatability was provided by coefficient of variation (CV) as the standard deviation of the difference between two measurements divided by the mean of the two measurements (35). Between-day reproducibility was also addressed by the CV between the first measurement in the first day and the measurement in the second day. Comparison was made between rest and exercise using paired, 2-sided student t test. Significance was defined as $P < 0.05$.

RESULTS

The simulation plots (Fig. 3) show exponential decay of the errors with increased SNR. In this study, T_1-weighted images with the longest TI had SNRs of 60 –100 due to using surface coils. According to this simulation, the calculated SMBF error would reach up to approximate 150% at rest, but would be < 25% during the contraction.

All volunteers underwent MR measurements successfully. Based on the geometry of the pedal and pneumatic cylinder of the exercise device, as well as increased pressure when the pedal was full depressed, the isometric contraction was estimated as 25% of MVC.

Data from soleus and gastrocnemius muscle groups are shown in Table 1 along with calculated $SMVO_2$. The mean resting SMBF in soleus (first measurement) was 6.5 ± 2.0 ml/min/100g tissue and increased >7-fold during the sustained contraction to 47.9 ± 7.7 ml/min/100g tissue ($P < 0.05$). SMOEF also tended to increase (from 0.36 ± 0.05 at rest to 0.44 ± 0.15 during exercise), but this difference was not statistically significant. $SMVO_2$ increased from 0.43 ± 0.13 ml/min/100g at rest to 4.2 ± 1.5 ml/min/100 g during exercise ($P < 0.05$). Both $R2'$ and venous blood volume also significantly increased. In gastrocnemius muscle, the data was similar except that SMOEF increased more than in soleus muscle, i.e., from 0.38 ± 0.04 and 0.58 ± 0.20, although this difference was not significant. Unlike $R2'$ and venous blood volume in soleus muscle, these parameters increased much less from resting to contracted states. In a comparison of these parameters between soleus and gastrocnemius muscle, only the resting venous blood volume shows significant difference ($P < 0.05$), although SMOEF appears to increase more in gastrocnemius muscle during contraction than in soleus muscle ($P = NS$).

NIH-PA Author Manuscript

NIH-PA Author Manuscript

NIH-PA Author Manuscript

The within-session repeatability between two measurements ranged mostly from excellent (<5%) to good (between 10% and 20%), for ROI measurements in both soleus and gastrocnemius groups, at rest and during contraction. SMOEF measurements had the best CV range, from 2.6% to 10.3%. As expected, CV of SMBF measurements was from 7.1% to 26.3%, perhaps due to some minor motion during the sustained contraction. This resulted in good to acceptable CV for $SMVO_2$ calculation (from 6.6 to 21.3%). The between-day reproducibility results of SMBF, SMOEF, and $SMVO_2$ are shown in Table 2. In the similar fashion as the repeatability, excellent to good reproducibility was observed for both soleus and gastrocnemius groups. Figure 4 shows sample images from one subject, demonstrating the regional distribution of SMBF and SMOEF, at rest and during sustained isometric contraction.

DISCUSSION AND CONCLUSION

This is the first non-invasive MRI oximetry developed for absolute quantification of regional skeletal muscle O_2 consumption. The feasibility of detecting regional differences in muscle perfusion and O_2 consumption was demonstrated in healthy volunteers through sustained isometric exercise, with good within-session repeatability. It was observed that blood flow in calf muscle increased up to 9-fold during sustained contraction at a moderate intensity of 25% MVC to approximately 40–60 ml/100g/min. This is similar to the peak post exercise SMBF of the calf (50 ml/100g/min) at 30% MVC reported by Richardson et al (36) using strain gauge plethysmograph. This increase in SMBF was accompanied by a tendency for a moderate (i.e., 20–50%) albeit non-statistically significant increase in muscle SMOEF. Few reports measured SMOEF in lower extremities. Using PET modality, resting SMOEF of the vastus intermedius muscle was 0.31 ± 0.16 in 12 young volunteers (37) and increased to 0.45 ± 0.11 during a 60-min intermittent isometric contraction at 10% MVC. However, SMOEF does not appear to have been previously measured in calf muscle at a similar contraction force (25% MVC).

There is a variation in the literature about resting calf blood flow. Snell et al (38) reported resting SMBF in the calf to be between 5.5 to 6.6 ml/100g/min. In a separate study (33), the resting calf blood flow was about 4–5 ml/100g/min in young healthy volunteers, but Boushel et al (39), using the same technique to measure resting calf blood flow, observed a value of 2.6 ± 0.3 ml/100g/min. This is consistent with the measurement obtained using a dye-dilution and near-infrared spectroscopy method (2.4 ± 0.2 ml/100g/min) by the same investigator (40). Based on these literature values of resting SMBFs, the averaged resting SMBF is approximately 4.3 ml/100g/min. However, these methods measured global leg blood flow, rather than regional microvascular blood flow. By injecting ^{15}O-water tracer, PET measurement provided a mean resting value of 3.12 ± 1.55 ml/100g/min in the femoral muscle of 18 young volunteers (41).

While the first-pass contrast enhanced MRI perfusion imaging can be adapted to measure SMBF (42,43), ASL has been extensively used in skeletal muscle research for the measurement of absolute blood flow with spatially and temporally resolved resolutions (26,44). In our study, we applied an empirically determined threshold (1–12 ml/100g/min) in the ROIs of SMBF maps to measure resting SMBF. The number of pixels within the threshold limit was typically 60–70% of non-zero pixel number in the ROI. The zero SMBF value represents very low blood flow that is beyond the detection limit of our ASL method (45). Typical resting SMBF in calf muscle measured by ASL were in the range of 8 – 30 ml/100g/min (20,25,46). The absolute values of resting SMBF in this study are in the lower end of that range, but still larger than those reported by non-MRI methods and the error agreed with what was predicted by our computer simulation (up to 150% error). Therefore, the overestimation of resting SMBF is likely to be caused mainly by relatively low SNR that

NIH-PA Author Manuscript

NIH-PA Author Manuscript

NIH-PA Author Manuscript

limits the accuracy of T_1 measurements in addition to other error sources, e.g., magnetization transit time, motion, and non-ideal RF pulse slice profile, etc. Methods to increase SNR are currently being investigated, including multiple data averaging, different signal acquisition schemes, and the usage of different receiver coils. Automatated postprocessing methods for the analysis of SMBF maps are also being investigated (44).

Regional skeletal muscle oxygen consumption has mostly been measured by NIRS and PET techniques. Because NIRS has limited penetration depth (< 1.5 cm) (47), only superficial muscle groups can be studied, e.g., gastrocnemius, biceps femoris, tibialis anterior, vastus lateralis, etc. PET requires relatively long scan time and involves radiation. In this study, there was approximately 10-fold increase in $SMVO_2$ from the resting state to the sustained contraction exercise (25% MVC). Heinonen et al (14) observed a 5–6-fold increase in $SMVO_2$ in thigh muscle during a 10% MVC exercise. The differences in the magnitude of the change may be attributed to different exercise protocols and muscle groups to be studied, in addition to measurement errors. Other studies have estimated skeletal muscle O_2 consumption from limb O_2 consumption determined using the arterio-venous balance approach (48,17), but as previously discussed it is difficult to directly compare them to our findings due to the difference in muscle groups involved and measurement methods (49).

The R2′ measured in this study match well with previously reported data (20), in which the resting R2′ was 5.4 s^{-1} and increased to approximately 9–10 s^{-1} during a 30% MVC isometric contraction. The resting venous blood volumes were 4% in gastrocnemius and 7% in soleus in this study. These blood volumes increased 75% and 100%, respectively, during the contraction. The resting gastrocnemius data is within the range of venous blood volume values in the literature. Coffman et al (46) used venous occlusion plethysmography to measure total calf venous volume and obtained 4.3–4.6%. Although PET and MRI can quantify regional absolute blood volume in tissue (50,51), there is no report about blood volume measurement in calf muscle with PET or MRI. With inhaled (^{15}O)CO, PET measurements yielded resting femoral muscle blood volume of approximately 4.3 ± 0.5 % in young untrained volunteers (52). If the ratio of venous blood volume to total blood volume in skeletal muscle is 0.75 (53), then the resting venous blood volume in femoral muscle would be 3.2%. Given the great flow heterogeneity in skeletal muscle, our calf muscle venous blood volume cannot be directly compared. Nevertheless, an interesting finding in this PET study is that there is no change in the venous blood volume during intermittent isometric exercise. In contrast, by using microbubble-enhanced ultrasound technique, it was found that blood volume in the vastus lateralis muscle increased 170 – 310% after 5-min knee-extensor exercise at different workloads (48). Again, these differences in the changes of blood volume among different studies may be attributed to different exercise protocols and muscle groups studied. Further investigations are warranted to fully understand the dynamic alternations of blood volume in skeletal muscle in healthy subjects and patients with peripheral diseases.

Despite differences in muscle fiber type and metabolism in the soleus and gastrocnemius muscles, there was no significant different in SMBF between them, at rest or during sustained contraction. Nevertheless, the significantly lower resting venous blood volume in gastrocnemius muscle may indicate lower capillary volume in the more fast-twitch muscles. There was also a tendency for SMOEF during sustained contraction to be higher in the gastrocnemius than in soleus. McDonough et al (54) observed similar greater oxygen extraction fraction in fast-twitch muscle than in slow-twitch soleus muscle during submaximal contractions in rats. Combining these methods with ^{31}P MR spectroscopy may provide more insight into oxidative and anaerobic metabolism in different types of skeletal muscle.

NIH-PA Author Manuscript

NIH-PA Author Manuscript

NIH-PA Author Manuscript

The between-day measurements for SMOEF at rest were fairly reproducible (4–9%), and the corresponding reproducibility was still acceptable (7.8 to 13.6%) for the sustained isometric exercise. These results are slightly better than reproducibility of baseline T2* measurements (12.3%) at rest or the dynamic BOLD measurements (21.5%) in a study of healthy volunteers (19), although two studies measured different image parameters for assessing muscle oxygenation. Different imaging and exercise protocols may explain the discrepancy in the reproducibility findings. In comparison with SMOEF measurements, SMBF reproducibility was slightly poorer (7–16.3%). This is consistent with the findings in the same study (19) that BOLD MRI had better interscan reproducibility than perfusion MRI using the dynamic contrast-enhanced technique. The underlying mechanism is unclear but may be related to relatively stable oxygenation and large day-to-day variations in muscle mircrocirculation. Of note, the within-session repeatability had similar performance for SMOEF and SMBF, except that SMBF in gastrocnemius muscle during the exercise fluctuated more within the same imaging session than SMBF between different days. One possible reason is the short 4-min interscan break time to allow gastrocnemius muscle to return to the baseline after one exercise. Nevertheless, it is warranted to have a large number of subjects to perform statistically meaningful measurements of the repeatability and reproducibility of this skeletal muscle oximetry technique.

Several limitations exist for the current techniques. The measurement of SMOEF is derived from a model used to calculate brain tissue OEF with the magnetic susceptibility effect of deoxyhemoglobin. This brain model assumed a random orientation of venous vessels. In skeletal muscle, the vessel orientation is rather parallel to the muscle fiber (55), at an angle θ relative to B_o. Because the vessel orientation affects the susceptibility effect, more accurate calculation of SMOEF needs to be derived from a model that accounts for the venous structure in skeletal muscle. Another limitation of this approach is that the OEF sequence is sensitive to the SNR of the images, resulting in the artifacts shown in the SMOEF maps (the arrow in Fig. 4). There is an ongoing effort to solve these problems in the current technical development phase. A rigorous validation study, perhaps using an animal model, may be needed in the future. Nevertheless, these issues appear less significant, given the fact that estimated SMOEF at rest and during exercise appears to be consistent with expected values in the calf muscle.

One potential source of susceptibility-weighted signal is from deoxymyoglobin that has the same haeme structure to hemoglobin. However, there are two reasons that we did not consider myoglobin modeling in this study. First, our model extracts signals from susceptibility changes in skeletal muscle, mainly from concentrated deoxyhemoglobin inside the vascular space, approximately 5–10% of muscle. Although myoglobin has the same amount of heame per unit mass of muscle, it is diluted over 80% intracellular space. Therefore, myoglobin concentration in muscle is approximately only 0.5 mM, substantially lower than hemoglobin concentration 5.18 mM of muscle blood at rest (56). For this reason, susceptibility effects from deoxymyoglobin generated local field perturbation should be very small. In fact, a study in skeletal muscle of human volunteers suggested that susceptibility effects in muscle were primarily from deoxyhemoglobin in the vascular space (57). However, the impact of deoxymyoglobin to the T_2 or R_2' is still unknown and is a logical area to be explored in detail. Second, in that study (56), myoglobin desaturation was estimated with *in vivo* proton NMR spectroscopy. Using an acute ischemia model, myoglobin desaturation reached a plateau after 5–7 min of onset ischemia. It was suggested that cell oxidative metabolism can be maintained through the release of oxygen from oxyhemoglobin (43) before this plateau. From a physiological point of view, the moderate isometric exercise in our study is unlikely to de-saturate significant amounts of oxygenated myoglobin within the measurement time (6 min). This can be partially explained by non-significant increase in oxygen extraction fraction, primarily from vascular origin.

NIH-PA Author Manuscript

NIH-PA Author Manuscript

NIH-PA Author Manuscript

Nevertheless, myoglobin contribution should be taken into account in our modeling and will be one of main subjects to be investigated in our laboratory.

Another challenge is the motion artifacts associated with exercise. In our study, only sustained contraction was prescribed so that minimal motion was present at rest or during the exercise. However, most exercise programs for assessing hemodynamics of skeletal muscle involve dynamic movement of the muscle. Measurements of SMBF and SMOEF take several seconds to minutes, which make them sensitive to subject motion. One way to overcome this difficulty is to synchronize the measurements to the periodic movement of the muscle, in a similar way to data acquisition during diastole in cardiac imaging. This is also an ongoing project in our laboratory.

In summary, the feasibility of non-invasive measurements of regional skeletal muscle perfusion and oxygen consumption has been demonstrated in normal volunteers. While further refinement and optimization are necessary for robust clinical application, these techniques have great potential to allow investigations of heterogeneity and coupling of local muscle blood flow and oxygen metabolism (32). It could also become a clinically valuable tool in the diagnosis and management of patients with altered skeletal muscle hemodynamics. In addition, a broad range of medical conditions could benefit from these techniques, including cardiology, gerontology, kinesiology, and physical therapy.

Acknowledgments

Research reported in this publication was supported by the Washington University Institute of Clinical and Translational Sciences grant UL1 TR000448 from the National Center for Advancing Translational Sciences (NCATS) of the National Institutes of Health (NIH). The content is solely the responsibility of the authors and does not necessarily represent the official view of the NIH

References

1. Zurlo F, Larson K, Bogardus C, Ravussin E. Skeletal muscle metabolism is a major determinant of resting energy expenditure. J Clin Invest. 1990; 86:1423–1427. [PubMed: 2243122]
2. Schrauwen P, Xia J, Bogardus C, Pratley RE, Ravusson E. Skeletal muscle uncoupling protein 3 expression is a determinant of energy expenditure in Pima Indians. Diabetes. 1999; 48:146–149. [PubMed: 9892236]
3. Conley KE, Amara CE, Jubrias SA, Marcinek DJ. Mitochondrial function, fibre types, and ageing: new insights from human muscle *in vivo*. Exp Physiol. 2007; 92:333–339. [PubMed: 17170059]
4. Amara CE, Shankland EG, Jubrias SA, Marcinek DJ, Kushmerick MJ, Conley KE. Mild mitochondrial uncoupling impacts cellular aging in human muscle *in vivo*. PNAS. 2007; 105:1057–1062. [PubMed: 17215370]
5. McConnell AK, Davies CT. A comparison of the ventilatory responses to exercise of elderly and younger humans. J Gerontol. 1992; 47:B137–141. [PubMed: 1624690]
6. Woo JS, Derleth C, Stratton JR, Levy WC. The influence of age, gender, and training on exercise efficiency. J Am Coll Cardiol. 2006; 47:1048–1057.
7. Levy WC, Maichel BA, Steele NP, Leclerc KM, Stratton JR. Biomechanical efficiency is decreased in heart failure during low-level steady state and maximal ramp exercise. Eur J Heart Fail. 2004; 6:917–926. [PubMed: 15556054]
8. Witte KK, Levy WC, Lindsay KA, Clark AL. Biomechanical efficiency is impaired in patients with chronic heart failure. Eur J Heart Fail. 2007; 9:834–838. [PubMed: 17569581]
9. Neder JA, Nery LE, Andreoni S, Sachs A, Whipp BJ. Oxygen cost for cycling as related to leg mass in males and females, aged 20 to 80. Int J Sports Med. 2000; 21:263–269. [PubMed: 10853697]
10. Lafortuna CL, Proiette M, Agosti F, Sartorio A. The energy cost of cycling in young obese women. Eur J Appl Physiol. 2006; 97:16–25. [PubMed: 16463044]

NIH-PA Author Manuscript

NIH-PA Author Manuscript

NIH-PA Author Manuscript

11. Mottram RF. The relationship between blood flow, arterio-venous oxygen difference, and oxygen uptake of human skeletal muscle. J Physiol. 1955; 130:42–43P. [PubMed: 13278935]
12. Coggan AR, Spina RJ, King DS, Rogers MA, Brown M, Nemeth PM, Holloszy JO. Skeletal muscle adaptations to endurance training in 60- to 70-yr-old men and women. J Appl Physiol. 1992; 72:1780–1786. [PubMed: 1601786]
13. Costes F, Barthélémy JC, Féasson L, Busso T, Geyssant A, Denis C. Comparison of muscle near-infrared spectroscopy and femoral blood gases during steady-state exercise in humans. J Appl Physiol. 1996; 80:1345–1350. [PubMed: 8926265]
14. Heinonen I, Saltin B, Kemppainen J, Sipilä HT, Oikonen V, Nuutila P, Knuuti J, Kalliokoski K, Hellsten Y. Skeletal muscle blood flow and oxygen uptake at rest and during exercise in humans: a PET study with nitric oxide and cyclooxygenase inhibition. Am J Physiol Heart Circ Physiol. 2011; 300:H1510–H1517. [PubMed: 21257921]
15. Carlier PG. Skeletal muscle perfusion and oxygenation assessed by dynamic NMR imaging and spectroscopy. Adv Exp Med Biol. 2011; 701:341–346. [PubMed: 21445807]
16. Schulte AC, Aschwanden M, Bilecen D. Calf muscles at blood oxygen level-dependent MR imaging: aging effects at postocclusive reactive hyperemia. Radiology. 2008; 247:482–489. [PubMed: 18372453]
17. Damon BM, Wadington MC, Hornberger JL, Lansdown DA. Absolute and relative contributions of BOLD effects to the muscle functional MRI signal intensity time course: effect of exercise intensity. Magn Reson Med. 2007; 58:335–345. [PubMed: 17654591]
18. Noseworthy MD, Bulte DP, Alfonsi J. BOLD magnetic resonance imaging of skeletal muscle. Semin Musculoskelet Radiol. 2003; 7:307–315. [PubMed: 14735429]
19. Versluis B, Backes WH, van Eupen MG, Jaspers K, Nelemans PJ, Rouwet EV, Teijink JA, Mali WP, Schurink GW, Wildberger JE, Leiner T. Magnetic resonance imaging in peripheral arterial disease: reproducibility of the assessment of morphological and functional vascular status. Invest Radiol. 2011; 46:11–24. [PubMed: 21102349]
20. Langham MC, Wehrli FW. Simultaneous mapping of temporally-resolved blood flow velocity and oxygenation in femoral artery and vein during reactive hyperemia. J Cardiovasc Magn Reson. 2011; 13:66–73. [PubMed: 22035402]
21. Elder CP, Cook RN, Chance MA, Copenhaver EA, Damon BM. Image-based calculation of perfusion and oxyhemoglobin saturation in skeletal muscle during submaximal isometric contractions. Magn Reson Med. 2010; 64:852–861. [PubMed: 20806379]
22. Yablonskiy DA, Haacke EM. Theory of NMR signal behavior in magnetically inhomogeneous tissues: the static dephasing regime. Magn Reson Med. 1994; 32:749–763. [PubMed: 7869897]
23. An H, Lin W. Quantitative measurements of cerebral blood oxygen saturation using magnetic resonance imaging. J Cereb Blood Flow Metab. 2000; 20:1225–1236. [PubMed: 10950383]
24. An H, Lin W. Impact of intravascular signal on quantitative measures of cerebral oxygen extraction and blood volume under normo- and hypercapnic conditions using an asymmetric spin echo approach. Magn Reson Med. 2003; 50:708–716. [PubMed: 14523956]
25. Spees WM, Yablonskiy DA, Oswood MC, Ackerman JJ. Water proton MR properties of human blood at 1.5 Tesla: magnetic susceptibility, T(1), T(2), T*(2), and non-Lorentzian signal behavior. Magn Reson Med. 2001; 45:533–542. [PubMed: 11283978]
26. Boss A, Martirosian P, Claussen CD, Schick F. Quantitative ASL muscle perfusion imaging using a FAIR-TrueFISP technique at 3.0 T. NMR Biomed. 2006; 19:125–132. [PubMed: 16404727]
27. Wu WC, Wang J, Detre JA, Wehrli FW, Mohler E 3rd, Ratcliffe SJ, Floyd TF. Hyperemic flow heterogeneity within the calf, foot, and forearm measured with continuous arterial spin labeling MRI. Am J Physiol Heart Circ Physiol. 2008; 294:H2129–H2136. [PubMed: 18310508]
28. Raynaud JS, Duteil S, Vaughan JT, Hennel F, Wary C, Leroy-Willig A, Carlier PG. Determination of skeletal muscle perfusion using arterial spin labeling NMRI: validation by comparison with venous occlusion plethysmography. Magn Reson Med. 2001; 46:305–311. [PubMed: 11477634]
29. Zhang H, Shea SM, Park V, Li D, Woodard PK, Gropler RJ, Zheng J. Accurate Myocardial T_1 Measurements: Toward Quantification of Myocardial Blood Flow with Arterial Spin Labeling. Magn Reson Med. 2005; 53:1135–1142. [PubMed: 15844151]

NIH-PA Author Manuscript

NIH-PA Author Manuscript

NIH-PA Author Manuscript

30. Kim SG. Quantification of relative cerebral blood flow change by flow-sensitive alternating inversion recovery (FAIR) technique: application to functional mapping. Magn Reson Med. 1995; 34:293–301. [PubMed: 7500865]

31. Belle V, Kahler E, Waller C, Rommel E, Voll S, Hiller KH, Bauer WR, Haase A. In vivo quantification of cardiac perfusion in rats using a noninvasive MR spin-labeling method. J Magn Reson Imaging. 1998; 8:1240–1245. [PubMed: 9848735]

32. Raitakari M, Nuutila P, Ruotsalainen U, Teräs M, Eronen E, Laine H, Raitakari OT, Iida H, Knuuti MJ, Yki-Järvinen H. Relationship between limb and muscle blood flow in man. J Physiol. 1996; 496:543–549. [PubMed: 8910236]

33. Alway SE, Coggan AR, Sproul MS, Abduljalil AM, Robitaille PM. Muscle torque in young and older untrained and endurance-trained men. J Gerontol A Biol Sci Med Sci. 1996; 51:B195–201. [PubMed: 8630695]

34. Nådland IH, Walløe L, Toska K. Effect of the leg muscle pump on the rise in muscle perfusion during muscle work in humans. Eur J Appl Physiol. 2009; 105:829–841. [PubMed: 19125282]

35. Bland JM, Altman DG. Measurement error. BMJ. 1996; 313:744. [PubMed: 8819450]

36. Richardson D, Shewchuk R. Effects of contraction force and frequency on post exercise hyperemia in human calf muscles. J Appl Physiol. 1980; 49:649–654. [PubMed: 7440279]

37. Kalliokoski KK, Knuuti J, Nuutila P. Blood transit time heterogeneity is associated to oxygen extraction in exercising human skeletal muscle. Microvasc Res. 2004; 67:125–132. [PubMed: 15020203]

38. Snell ES, Eastcott HH, Hamilton M. Circulation in lower limb before and after reconstruction of obstructed main artery. Lancet. 1960; 1:242. [PubMed: 13832271]

39. Boushel R, Langberg H, Green S, Skovgaard D, Bulow J, Kjaer M. Blood flow and oxygenation in peritendinous tissue and calf muscle during dynamic exercise in humans. J Physiol. 2000; 524:305–313. [PubMed: 10747200]

40. Boushel R, Langberg H, Olesen J, Nowak M, Simonsen L, Bülow J, Kjaer M. Regional blood flow during exercise in humans measured by near-infrared spectroscopy and indocyanine green. J Appl Physiol. 2000; 89:1868–1878. [PubMed: 11053338]

41. Ruotsalainen U, Raitakari M, Nuutila P, Oikonen V, Sipilä H, Teräs M, Knuuti MJ, Bloomfield PM, Iida H. Quantitative blood flow measurement of skeletal muscle using oxygen-15-water and PET. 1997; 38:314–319.

42. Thompson RB, Aviles RJ, Faranesh AZ, Raman VK, Wright V, Balaban RS, McVeigh ER, Lederman RJ. Measurement of skeletal muscle perfusion during post ischemic reactive hyperemia using contrast-enhanced MRI with a step-input function. Magn Reson Med. 2005; 54:289–298. [PubMed: 16032661]

43. Isbell DC, Epstein FH, Zhong X, DiMaria JM, Berr SS, Meyer CH, Rogers WJ, Harthun NL, Hagspiel KD, Weltman A, Kramer CM. Calf muscle perfusion at peak exercise in peripheral arterial disease: measurement by first-pass contrast-enhanced magnetic resonance imaging. J Magn Reson Imaging. 2007; 25:1013–1020. [PubMed: 17410566]

44. Carlier PG, Bertoldi D, Baligand C, Wary C, Fromes Y. Muscle blood flow and oxygenation measured by NMR imaging and spectroscopy. NMR Biomed. 2006; 19:954–967. [PubMed: 17075963]

45. Frouin F, Duteil S, Lesage D, Carlier PG, Herment A, Leroy-Willig A. An automated image-processing strategy to analyze dynamic arterial spin labeling perfusion studies. Application to human skeletal muscle under stress. Magn Reson Imaging. 2006; 24:941–951. [PubMed: 16916711]

46. Frouin F, Duteil S, Lesage D, Carlier PG, Herment A, Leroy-Willig A. An automated image-processing strategy to analyze dynamic arterial spin labeling perfusion studies. Application to human skeletal muscle under stress. Magn Reson Imaging. 2006; 24:941–951. [PubMed: 16916711]

47. Ferrari M, Muthalib M, Quaresima V. The use of near-infrared spectroscopy in understanding skeletal muscle physiology: recent developments. Philos Transact A Math Phys Eng Sci. 2011; 369:4577–4590.

NIH-PA Author Manuscript

NIH-PA Author Manuscript

NIH-PA Author Manuscript

48. Sørlie D, Myhre K, Mjøs OD. Exercise-and post-exercise metabolism of the lower leg in patients with peripheral arterial insufficiency. Scand J Clin Lab Invest. 1978; 38:635–642. [PubMed: 715365]

49. van Hall G, González-Alonso J, Sacchetti M, Saltin B. Skeletal muscle substrate metabolism during exercise: methodological considerations. Proc Nutr Soc. 1999; 58:899–912. [PubMed: 10817157]

50. Martin WR, Powers WJ, Raichle ME. Cerebral blood volume measured with inhaled C15O and positron emission tomography. J Cereb Blood Flow Metab. 1987; 7:421–426. [PubMed: 3497162]

51. Lu H, Law M, Johnson G, Ge Y, van Zijl PC, Helpern JA. Novel approach to the measurement of absolute cerebral blood volume using vascular-space-occupancy magnetic resonance imaging. Magn Reson Med. 2005; 54:1403–1411. [PubMed: 16254955]

52. Kalliokoski KK, Oikonen V, Takala TO, Sipilä H, Knuuti J, Nuutila P. Enhanced oxygen extraction and reduced flow heterogeneity in exercising muscle in endurance-trained men. Am J Physiol Endocrinol Metab. 2001; 280:E1015–1021. [PubMed: 11350784]

53. Pollard V, Prough DS, DeMelo AE, Deyo DJ, Uchida T, Widman R. The influence of carbon dioxide and body position on near-infrared spectroscopic assessment of cerebral hemoglobin oxygen saturation. Anesth Analg. 1996; 82:278–287. [PubMed: 8561327]

54. McDonough P, Behnke BJ, Padilla DJ, Musch TI, Poole DC. Control of microvascular oxygen pressures in rat muscles comprised of different fibre types. J Physiol. 2005; 563:903–913. [PubMed: 15637098]

55. Mathieu-Costello O. Capillary tortuosity and degree of contraction or extension of skeletal muscles. rovasc Res. 1987; 33:98–117.

56. Lai N, Zhou H, Saidel GM, Wolf M, McCully K, Gladden LB, Cabrera ME. Modeling oxygenation in venous blood and skeletal muscle in response to exercise using near-infrared spectroscopy. J Appl Physiol. 2009; 106:1858–1874. [PubMed: 19342438]

57. Lebon V, Brillault-Salvat C, Bloch G, Leroy-Willig A, Carlier PG. Evidence of muscle BOLD effect revealed by simultaneous interleaved gradient-echo NMRI and myoglobin NMRS during leg ischemia. Magn Reson Med. 1998; 40:551–558. [PubMed: 9771572]

NIH-PA Author Manuscript
NIH-PA Author Manuscript
NIH-PA Author Manuscript

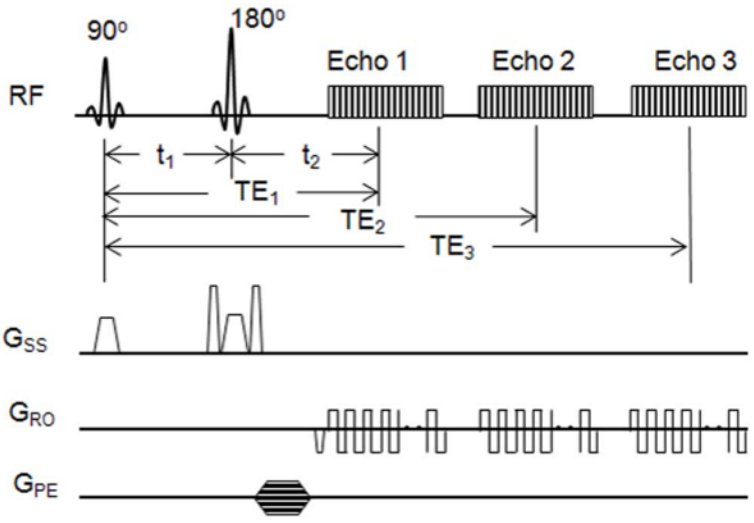

Figure 1.
Diagram of the 2D triple-echo asymmetric spin-echo sequence for the calculation of SMOEF. The timing parameters are defined in the text. G_{SS} = gradients along the slice-select direction, G_{RO}= gradients along the readout direction, G_{PE} = gradients along the phase-encoding direction.

NIH-PA Author Manuscript

NIH-PA Author Manuscript

NIH-PA Author Manuscript

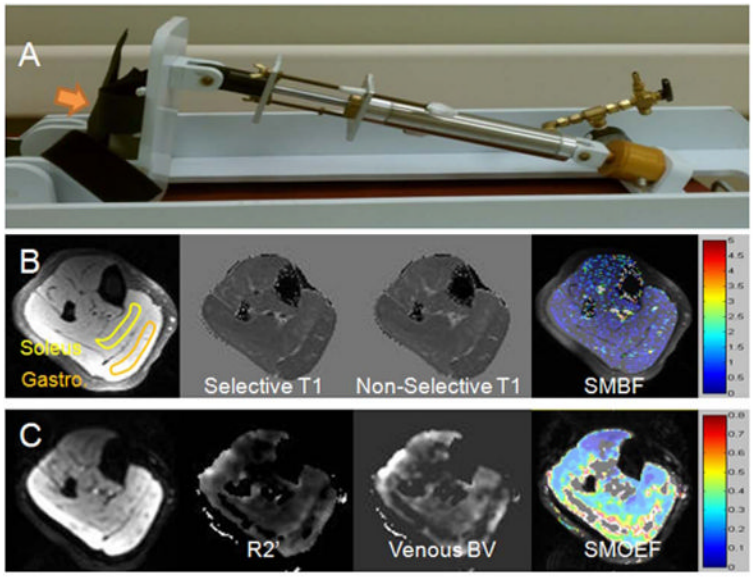

Figure 2.

Photos of home-made exercise device (A), images from ASL measurements (B), and images from SMOEF measurements (C). In panel A, an arrow points to the pedal for the leg contraction. In panel B, from left to right: source T_1-weighted image, selective T_1 map, non-selective T_1 map, and resulting SMBF map. In panel C, from left to right: source T_2'-weighted image, calculated R_2' map, calculated venous blood volume map, and SMOEF map. The two ROIs on the T_1-weighted image in panel B represent the regions in which measurements were obtained.

NIH-PA Author Manuscript

NIH-PA Author Manuscript

NIH-PA Author Manuscript

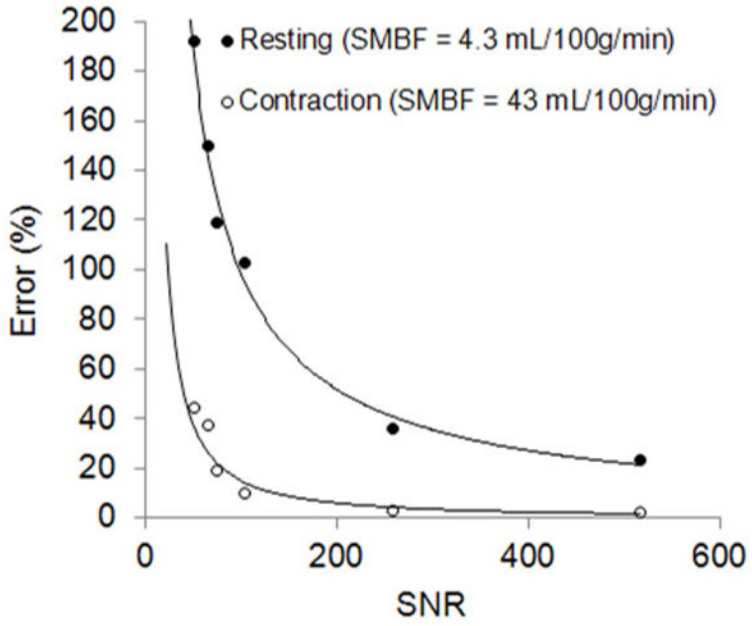

Figure 3.
Simulation of relationship between SNRs of source T_1-weighted images and the errors of calculated SMBF values, at two physiologic states: resting and leg contraction exercise.

NIH-PA Author Manuscript

NIH-PA Author Manuscript

NIH-PA Author Manuscript

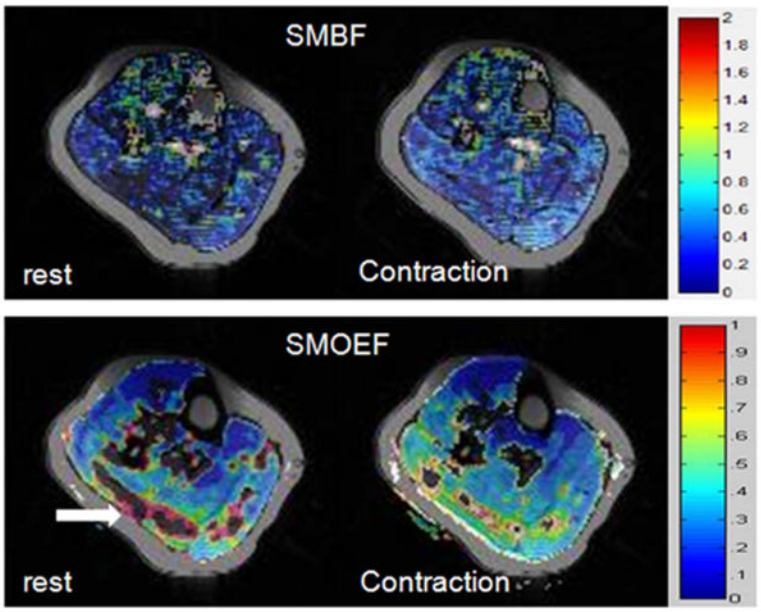

Figure 4.

SMBF (top row) and SMOEF (bottom row) maps of one volunteer at rest and during sustained contraction. Elevation in SMBF and SMOEF are demonstrated. The block arrow in resting SMOEF map points to the “artifacts” from the erroneous calculation of SMOEF. The color scale bar for SMBF: 0 – 2ml/g/min; for SMOEF: 0 – 1.

NIH-PA Author Manuscript NIH-PA Author Manuscript NIH-PA Author Manuscript

Table 1

Results of skeletal muscle perfusion and oxygen uptake with repeated measurements in two muscle groups (n = 5). #1 = the first measurement, #2 = the second measurement

Soleus						
	Baseline			Exercise		
	#1	#2	CV	#1	#2	CV
SMBF (ml/100g/min)	6.5 ± 2.0	6.7 ± 0.5	12.8%	47.9 ± 7.7*	53.1 ± 14.3*	13.2%
SMOEF	0.36 ± 0.05	0.36 ± 0.05	3.1%	0.44 ± 0.15	0.43 ± 0.18	7.5%
$SMVO_2$ (ml/100g/min)	0.43 ± 0.13	0.45 ± 0.1	13.9%	4.2 ± 1.5*	4.4 ± 2.6*	9.4%
R2′ (sec^{-1})	5.9 ± 2.0	6.1 ± 2.0	5.4%	9.9 ± 3.1*	9.3 ± 3.2	10.2%
Venous Blood Volume	7 ± 2 (%)	8 ± 2 (%)	5.6%	14 ± 6 (%)*	13 ± 8 (%)	17.1%

Gastrocnemius						
	Baseline			Exercise		
	#1	#2	CV	#1	#2	CV
SMBF (ml/100g/min)	6.9 ± 0.8	6.9 ± 1.0	7.1%	43.8 ± 16.2*	64.6 ± 20*	26.3%
SMOEF	0.38 ± 0.04	0.38 ± 0.04	2.6%	0.49 ± 0.2	0.47 ± 0.11*	8.4%
$SMVO_2$ (ml/100g/min)	0.48 ± 0.01	0.49 ± 0.07	6.7%	3.8 ± 2.5*	6.1 ± 2.9*	21.3%
R2′ (sec^{-1})	5.9 ± 3.5	6.2 ± 3.8	10.3%	7.2 ± 1.1	6.9 ± 1.6	9.5%
Venous Blood Volume	4 ± 2 (%)	4 ± 1 (%)	9.8%	7 ± 2 (%)*	7 ± 2 (%)*	20.1%

*(Two-tailed paired t-test) $P < 0.05$, Exercise #1 or #2 vs. Baseline #1 or #2

Magn Reson Med. Author manuscript; available in PMC 2015 January 01.

NIH-PA Author Manuscript

NIH-PA Author Manuscript

NIH-PA Author Manuscript

Table 2

Reproducibility of skeletal muscle perfusion and oxygen uptake

	CV (Baseline)		CV (Exercise)	
	Soleus	**Gastrocnemius**	**Soleus**	**Gastrocnemius**
SMBF	7.0%	7.0%	16.3%	14.0%
SMOEF	4.0%	9.0%	7.8%	13.6%
$SMVO_2$	6.4%	6.6%	8.9%	15.2%